Iraqi Journal of Science, 2020, Vol. 61, No. 2, pp: 389-400
DOI: 10.24996/ijs.2020.61.2.17

ISSN: 0067-2904

Disequilibrium Compaction, Fluid expansion and unloading effects: Analysis from well log and its pore pressure implication in Jay Field, Niger Delta

Abbey Chukwuemeka Patrick[1, 2]*, Meludu Chukwudi Osita[2], Oniku Adetola Sunday[2], Mamman Yusuf Dabari[1, 3]

[1]Department of Petroleum Chemistry & Physics, American University of Nigeria
[2]Department of Physics, Modibbo Adama University of Technology Yola
[3]Department of Geology, Modibbo Adama University of Technology Yola

Received: 24/6/ 2019 Accepted: 28/ 8/2019

Abstract

Disequilibrium compaction, sometimes referred to as under compaction, has been identified as a major mechanism of abnormal pore pressure buildup in sedimentary basins. This is attributed to the interplay between the rate at which sediments are deposited and the rate at which fluids associated with the sediments are expelled with respect to burial depth. The purpose of this research is to analyze the mechanisms associated with abnormal pore pressure regime in the sedimentary formation. The study area "Jay field" is an offshore Niger Delta susceptible to abnormal pore pressure regime in the Agbada –Akata formations of the basin. Well log analysis and cross plots were applied to determine the under compacted zone in the formation since compaction increases with burial depth. It was observed that porosity and permeability of the deeper depth (3700 m to end of Well) are higher than those of the shallow part (3000 – 3700 m). This is against what is expected from normal compacted sediment, demonstrating disequilibrium compaction in deposition. Furthermore, it reveals that sedimentation rate was high, making it unable for the sediments to expunge its fluid as expected. Density and acoustic wave increase with depth in normal compaction trend. However, the reverse that was identified in the mapped interval is attributed to disequilibrium compaction, unloading, clay diagenesis, and fluid expansion. The cross plot divulges sediments at the deeper depth had lower density and acoustic wave value with increased porosity when compared to those at shallow depth. This forms the basis that the sediments from this mapped interval experienced disequilibrium and unloading traceable to clay diagenesis during and after deposition, respectively.

Keywords: Disequilibrium, compaction, deposition, Sediments, pressure

Introduction

The process of sediment deposition, sedimentation, compaction and the rate at which the compacted (deposited) sediment losses its fluid is relevant in formation pore pressure studies. Pore pressure is the pressure associated with formation fluids in the subsurface and it varies from normal if the pore pressure of the formation is the same as the hydrostatic pressure and abnormal when it is below or above the hydrostatic pressure. This variation in pore pressure regime is associated with under-compaction, fluid expansion and migration, and tectonics [1].

Under-compaction is regarded as compaction disequilibrium that arises when the rate of deposition and burial are sufficiently high relative to the vertical permeability of sediments [2]. Disequilibrium

*Email: emexabbey@gmail.com

compaction commonly exists among young and rapidly buried sediments around the world. When the sediment deposition is at high rate, sediments tend to aggregate at a fast rate without losing their associated fluid with respect to depth. At this point, porosity fails to decrease and density, instead of increasing, experiences a decrease with respect to burial depth. These sediments in question are mostly shales /clays with low permeability, which makes it difficult for the sediments to lose their fluid at same rate of deposition since the rate of compaction is dependent on burial history and the lithology of the sediments. Under-compaction /disequilibrium compaction can be attributed to the inability or failure of mechanical and chemical activities that are responsible for keeping the formation pressure at hydrostatic pressure level.

Sediments compacts mechanically when there is a reduction in the volume of the formation associated with expulsion of fluids within the sediments due to increasing overburden weight. This brings about the re-arrangement (rotation, bending and fracturing) of grains leading to compactions of sediments that is driven by vertical effective stress from the increasing overburden [3]. An increase in temperature associated with depth of burial brings about mineral transformation which affects the physical composition of the sediments; this is conspicuous in the cementation of quartz. This means that chemical activities bring about further compaction processes after the mechanical activities has taken place.

Other mechanisms of abnormal pressure that are associated with temperature are clay diagenesis, aqua thermal expansion, source rock maturation, fluid migration, hydrocarbon generation from organic rich shale, and thermal cracking of oil to gas.

This work intends to delineate abnormal/ over pressured formation within the study field that is penetrated by a well log, in addition to the analysis of the mechanisms responsible for the abnormal pressure regime and the viability of cross plot in classification of other mechanisms in relation to disequilibrium compaction of sediments.

1.2 Geology of the Study Area

The field of study (Jay Field) is situated in the Niger Delta hydrocarbon province of West Africa (Figure-1). The province covers 300,000 km^2 and includes the geologic extent of the Tertiary Niger Delta (Akata - Agbada) Petroleum System [4].

The Delta Province contains only one identified petroleum system [5, 6] which is referred to as the Tertiary Niger Delta (Akata – Agbada) Petroleum System. The delta formed at the site is of a rift triple junction related to the opening of the southern Atlantic which started in the Late Jurassic, continued into the Cretaceous [7] and stopped in the Late Cretaceous. After rifting ceased, gravity tectonism became the primary deformational process. Shale mobility induced internal deformation and occurred in response to two processes [5]. First, shale diapirs formed from loading of poorly compacted, over-pressured, prodelta and delta-slope clays (Akata Formation) by the higher density delta-front sands (Agbada Formation). Second, slope instability occurred due to a lack of lateral basin ward support for the under-compacted delta-slope clays (Akata Formation). For any given depobelt, gravity tectonics were completed before deposition of the Benin Formation and are expressed in complex structures, including shale diapirs, roll-over anticlines, collapsed growth fault crests, back-to-back features, and steeply dipping, closely spaced flank faults [8, 9]. These faults mostly offset different parts of the Agbada Formation and flatten into detachment planes near the top of the Akata Formation [4].

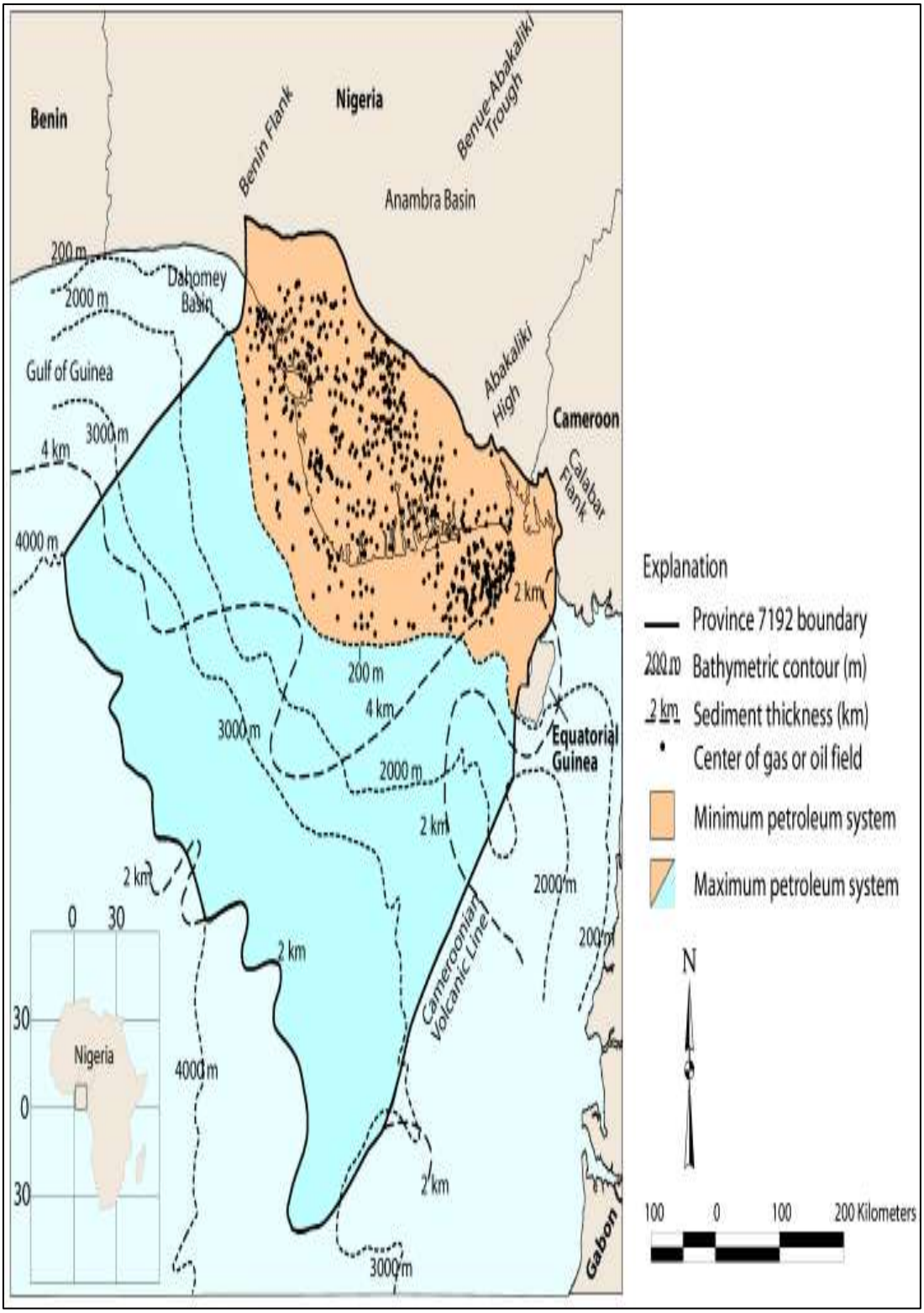

Figure 1-The Niger Delta Province Outline [4].

The stratigraphic evolution of the Tertiary Niger Delta (Figure-2) and the underlying Cretaceous strata were described by Short and Stauble [10]. The three major lithostratigraphic units defined in the subsurface of the Niger Delta (Akata, Agbada and Benin Formations) decrease in age basinward, reflecting the overall regression of depositional environments within the Niger Delta clastic wedge. The formations reflect a gross coarsening-upward progradational clastic wedge [10], deposited in marine, deltaic, and fluvial environments [11].

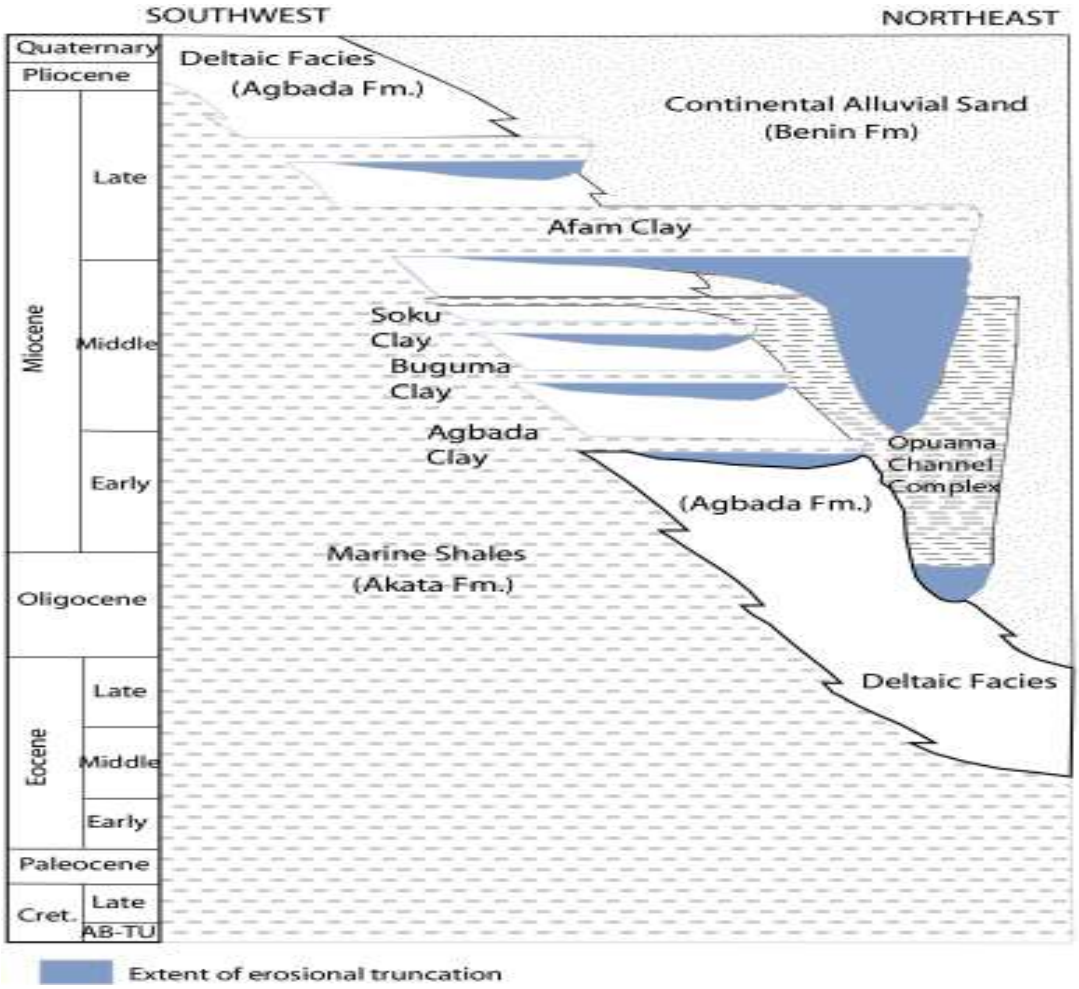

Figure 2-Stratigraphic Column showing Formations of the Niger Delta [12].

1.0 Materials and Method

The data were acquired from Chevron Nigeria through the department of petroleum Resources. The field of study, Jay field, has 3D seismic and one drilled Well that comprises gamma ray, resistivity, density, sonic wave, and neutron logs, as shown in figure 3.

The P-wave and S-wave velocities were determined using Ogagarue [13] localized Vp and Vs relationship model for Niger Delta sedimentary region.

$$V_P = 1.11702V_S + 1279.08 \quad (2.1)$$

$$V_P = 1000000 * \frac{0.305}{D_{tp}} \quad (2.2)$$

$$V_S = 1000000 * \frac{0.305}{D_{ts}} \quad (2.3)$$

Where D_{tp} and D_{ts} are the interval transit times recorded by the compressional and shear sonic logs, respectively, in μsec/ft.

Neutron – Density porosity was used in the analysis of porosity estimation. Density porosity was obtained from equation 2.4:

$$\phi_d = \frac{\rho_{matrix} - \rho_b}{\rho_{matrix} - \rho_f} \quad (2.4)$$

Where ρ_{matrix} is the rock matrix density (sandstone 2.65 g/cm^3 and Shale is within 2.63-2.66 g/cm^3), ρ_b is the bulk density from the log, ρ_f is the density of the fluids contained in the rock pore space (1.0, 1.1, 0.8, and 0.6 for freshwater, Salty water, oil and gas, respectively) and ϕ_d is the density porosity.

Neutron – Density porosity was estimated using the average in equations (2.5):

$$\phi_{nd} = \frac{\phi_n^2 + \phi_d^2}{2} \quad (2.5)$$

Permeability was determined using the Coates and Dumanoir [14] empirical formula by calculating the irreducible water saturation from equation 2.6 and inputting it in equation 2.7

$$S_{wir} = \left(\frac{1}{2000 \times \phi^2}\right)^{0.5} \quad 2.6$$

$$K = 4.90 \times \frac{\phi^4 (1 - S_{wir})^2}{S_{wir}^4} \quad 2.7$$

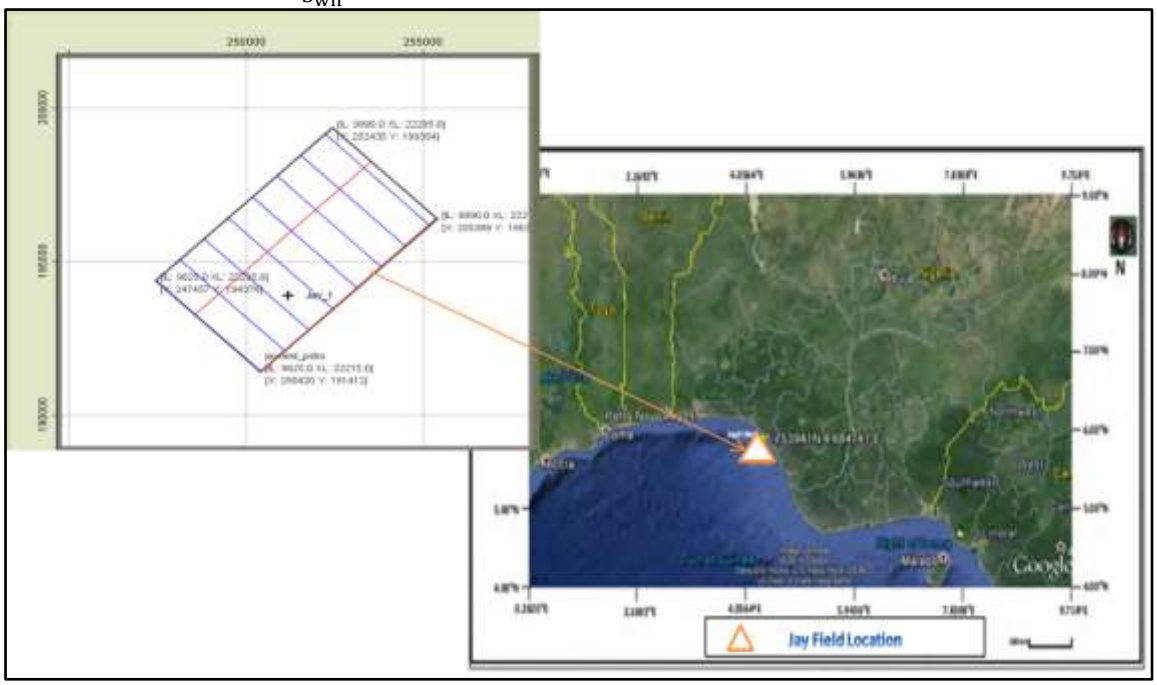

Figure 3-Location of the base map of the study field in Google map.

The cross plot guide in Figure-4 will assist in the classification of the causes of abnormal pore pressure mechanisms associated with the formation.

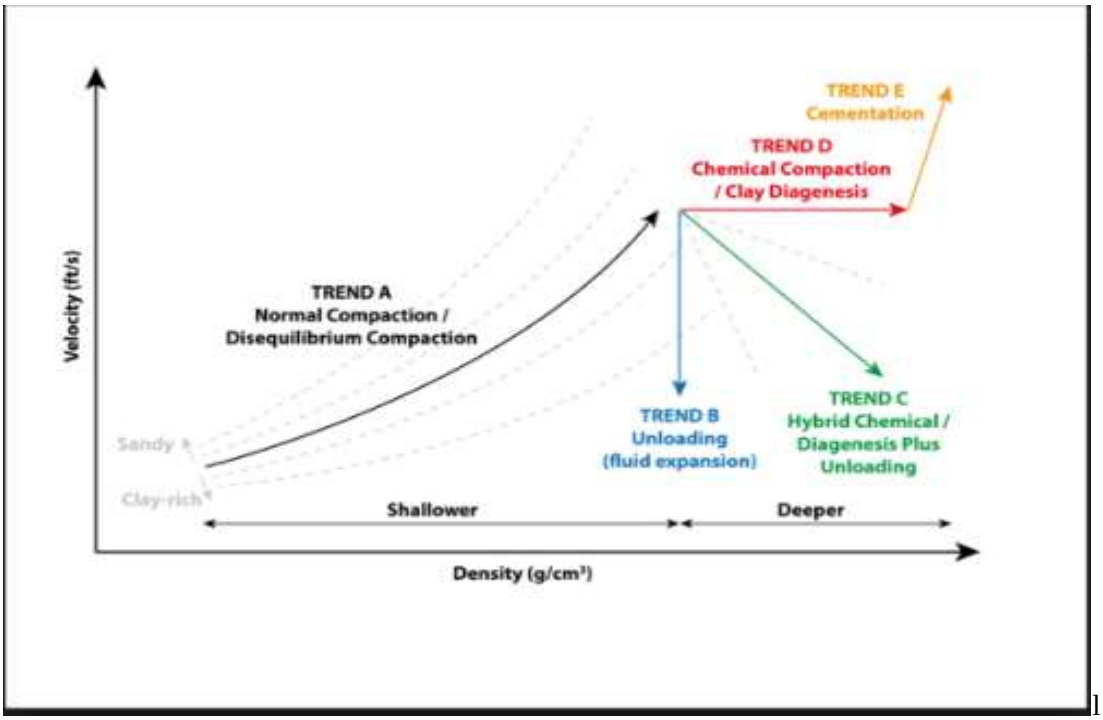

Figure 4-Velocity-Density crossplots with associated overpressure generating mechanisms [15].

2.Result and discussion

Figure-5 displays the well log view of gamma ray, resistivity, porosity, density, and the computed logs of p-wave and p-impedance. From the figure below, the yellowish and the gray portions of the gamma ray log depict the sand and shale sequence respectively. Just immediately after the last reservoir rock (low gamma and high value of the resistivity) comes the over pressure region in this field. At this point, there is a noticeable reversal in the trend line of the porosity, density and P-wave, with an increase in porosity which is a good indicator of pressurized zone since porosity decreases with depth. While the density, P-wave and P-impedance logs experience a sharp decrease throughout this region against the supposed increase since they are supposed to increase with depth. These are true representation of an abnormal pressure regime in this formation. In Figure-6, the normal compaction trend line estimated from Vp (P-wave) log discloses the deviation from normal pressure trend (hydrostatic pressure) to abnormal pressure regime. This implies that at the point of deviation from the trend line lies the onset of over pressure at the formation.

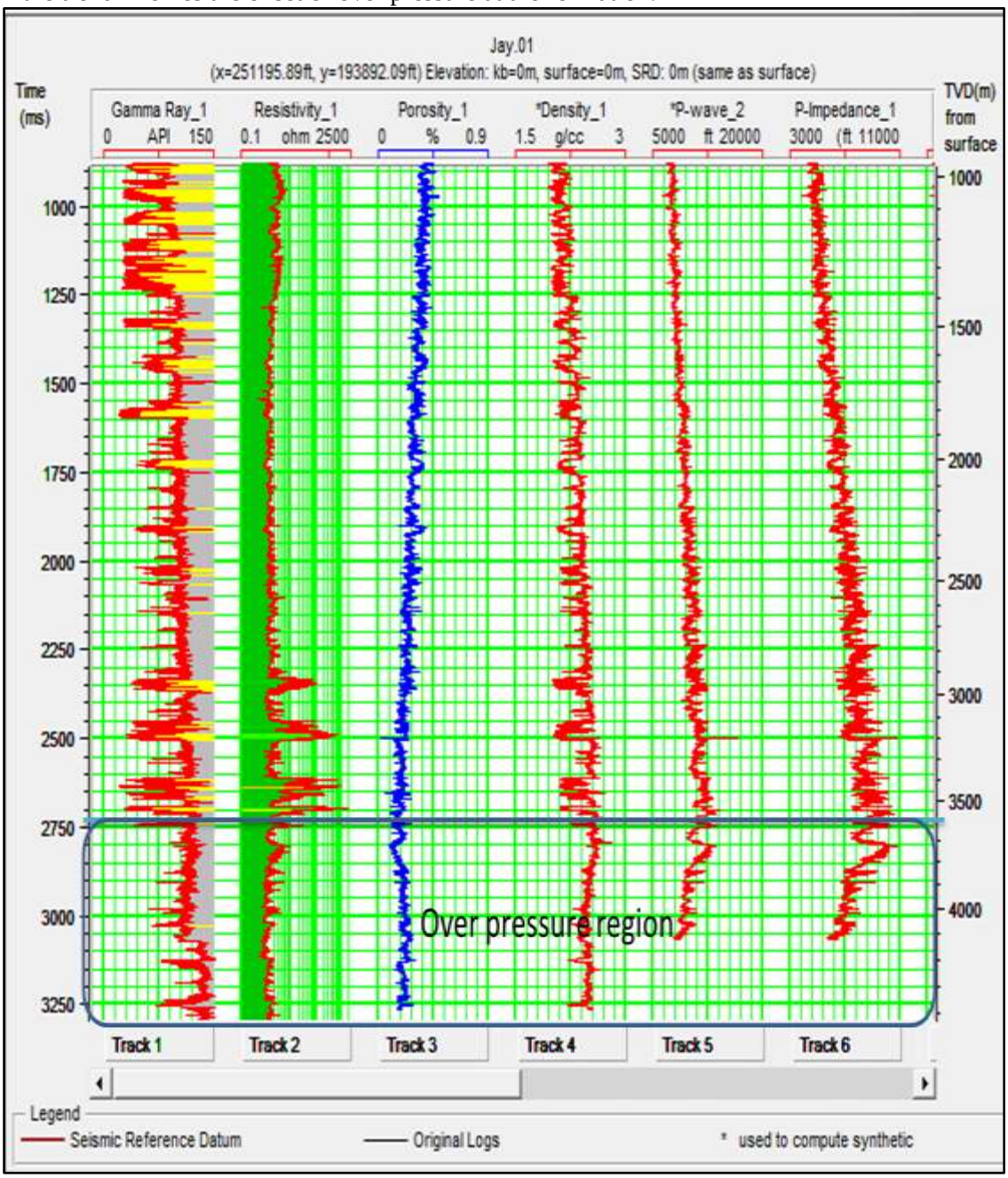

Figure 5-Well log view of Jay well, showing the over pressure region.

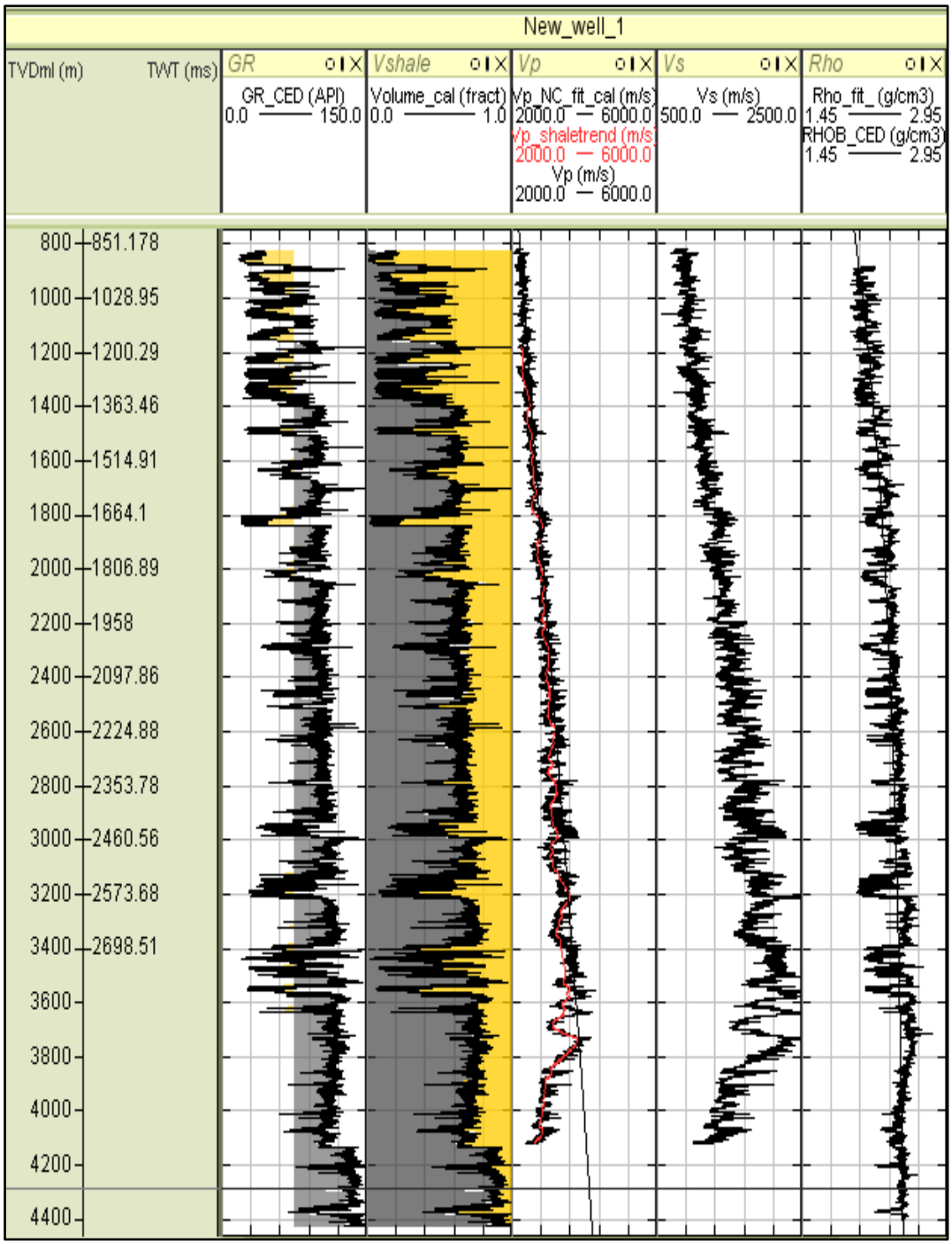

Figure 6-Display of Normal compaction trend line, Vp Shaletrend and Overburden gradient.

The cross plot of porosity against permeability in Figure-7 divulges an anomaly plot at the green oval spot. During burial, intrinsic permeability decreases with increasing depth due to the reduction in porosity. However, the dark blue area in the cross plot trend should have plotted before the lighter blue plot since the dark blue represent deeper depth (check the depth legend) compared to the former. In view of this, the porosity and permeability of the deeper depth (3700 m and above) is more than the shallow part (3000 – 3700 m), uncovering disequilibrium compaction during sedimentation. This shows that the rate at which sedimentation occurred was high, making it unable for the sediments to expunge its associated fluid as expected. Furthermore, the lithology of the formation enabled it to be so, since shales/clays has high ability to absorb fluids and its permeability is low.

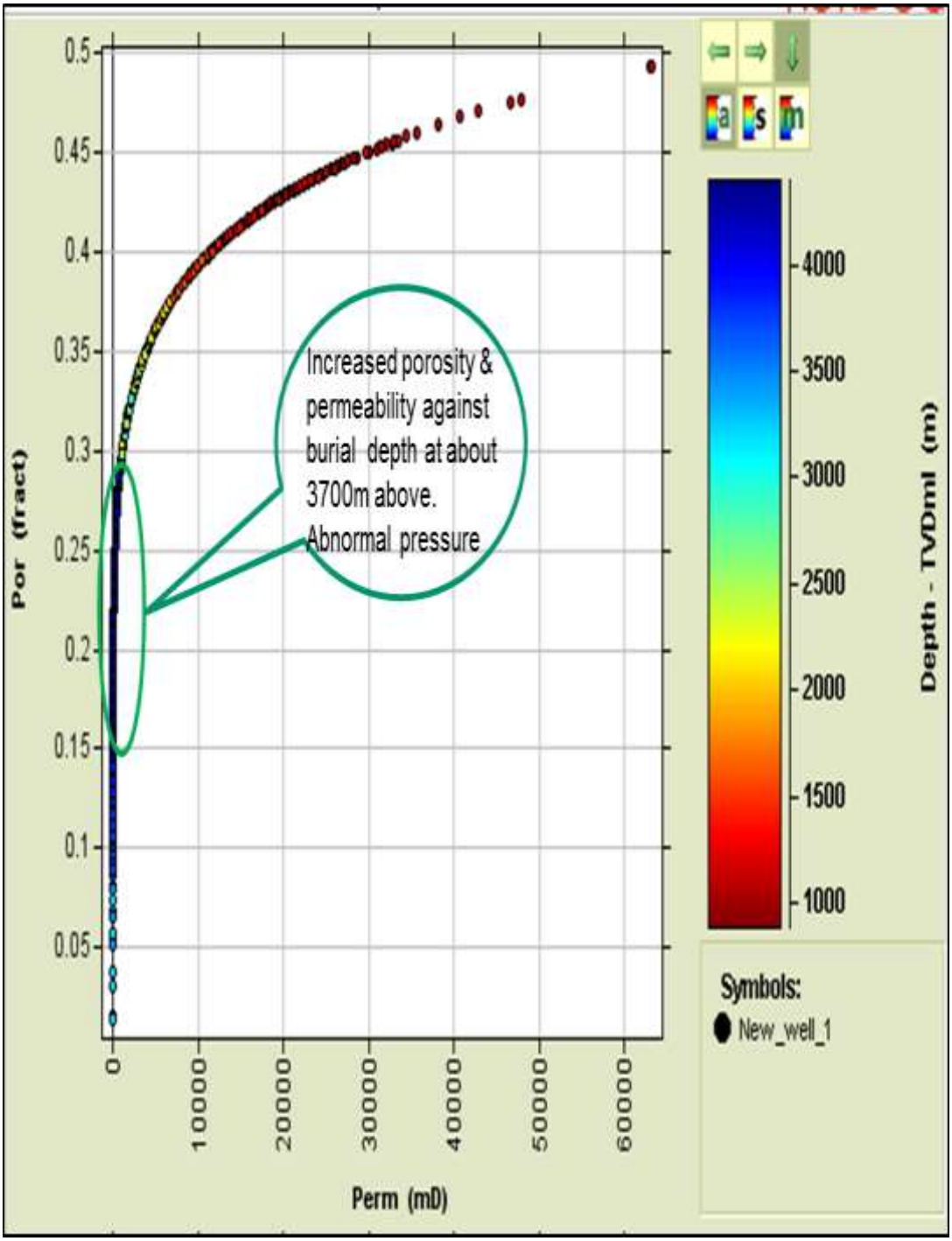

Figure 7-Cross plot of porosity against permeability showing abnormal pressure region.

P-wave and density increases with depth due to compaction of sediments in formations. This became conspicuous as observed in the cross plot of p-wave against density in Figure-8 from the top to the depth of about 3600 m before the anomalous change in trend as observed. From about 3600m to the depth penetrated by the well log, a drastic reduction in P-wave and density is revealed which is captured in the white circle as under compaction (Disequilibrium compaction). In normal situation (hydrostatic pressure) the sediments that are represented in the circle are supposed to have plotted at the position of the black arrow, since compaction increases with depth and the sound waves travel fast in densely compacted medium. Hence, the density of the sediments in the circled area is also expected to be high. In the second diagram of Figure-8 that is coloured by porosity log, the circled portion of the plot is having a high porosity value, which is against what is expected in a normal compaction formation; it is supposed to plot at the black arrow point since porosity decreases with depth. This

under compacted or disequilibrium compacted sediment was then isolated for further analysis in Figure-9.

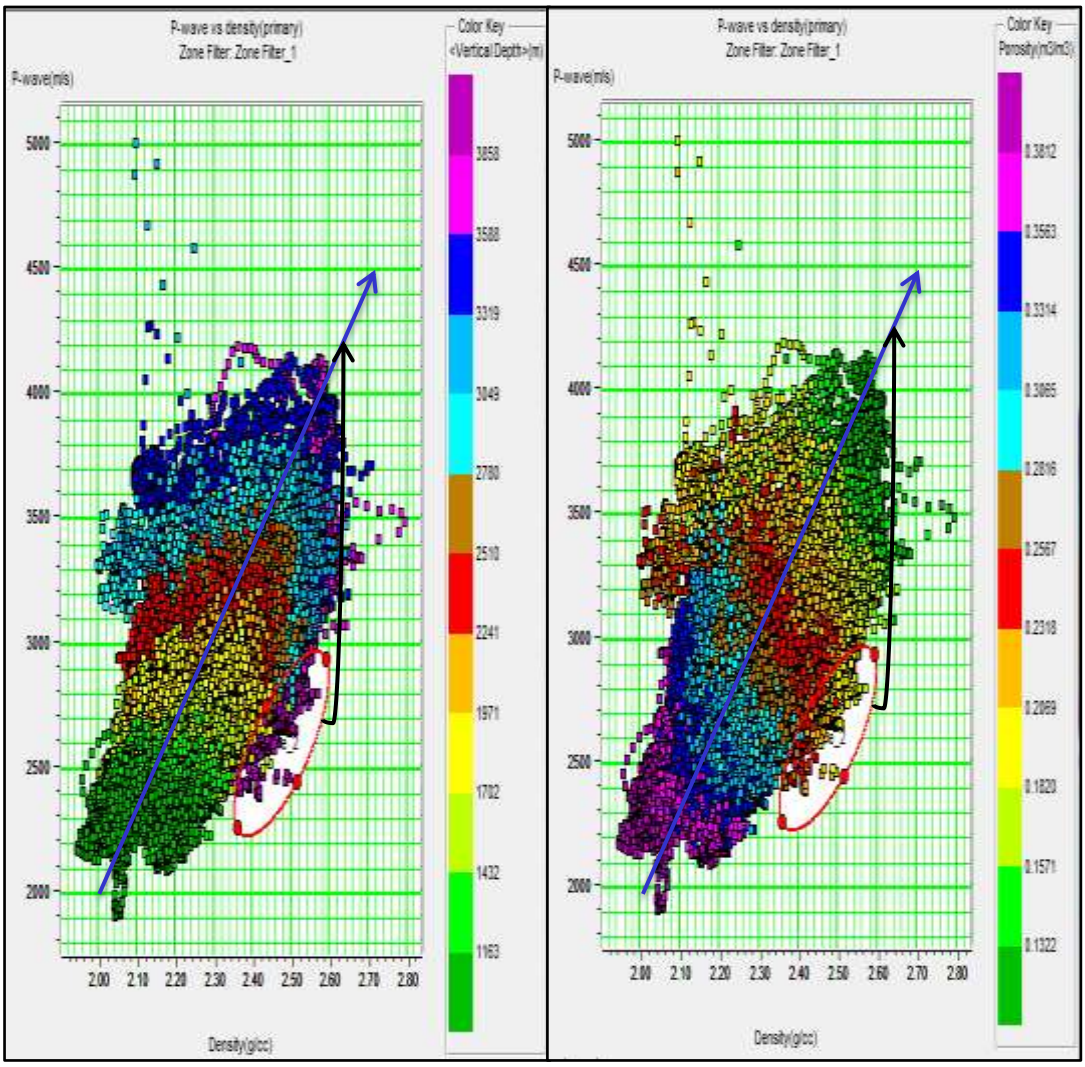

Figure 8-The cross plot of P-wave versus Density.

Figure-9 represents the cross plot of P- wave and density log for a plot of an interval of 3600 m to well end. This plot range covers the area marked with a white circle in Figure-8. The density and acoustic wave increase with depth in normal compaction trend. However, the reverse applies in this selected interval because of disequilibrium compaction, unloading, clay diagenesis and fluid expansion. From the color keys in the cross plot, sediments at deeper depth have a lower density and acoustic wave value with increased porosity when compared with those at shallow depth. This forms the basis that the sediments from this isolated interval experience disequilibrium compartment during deposition. The clusters in light blue seem to represent unloading that is due to clay diagenesis.

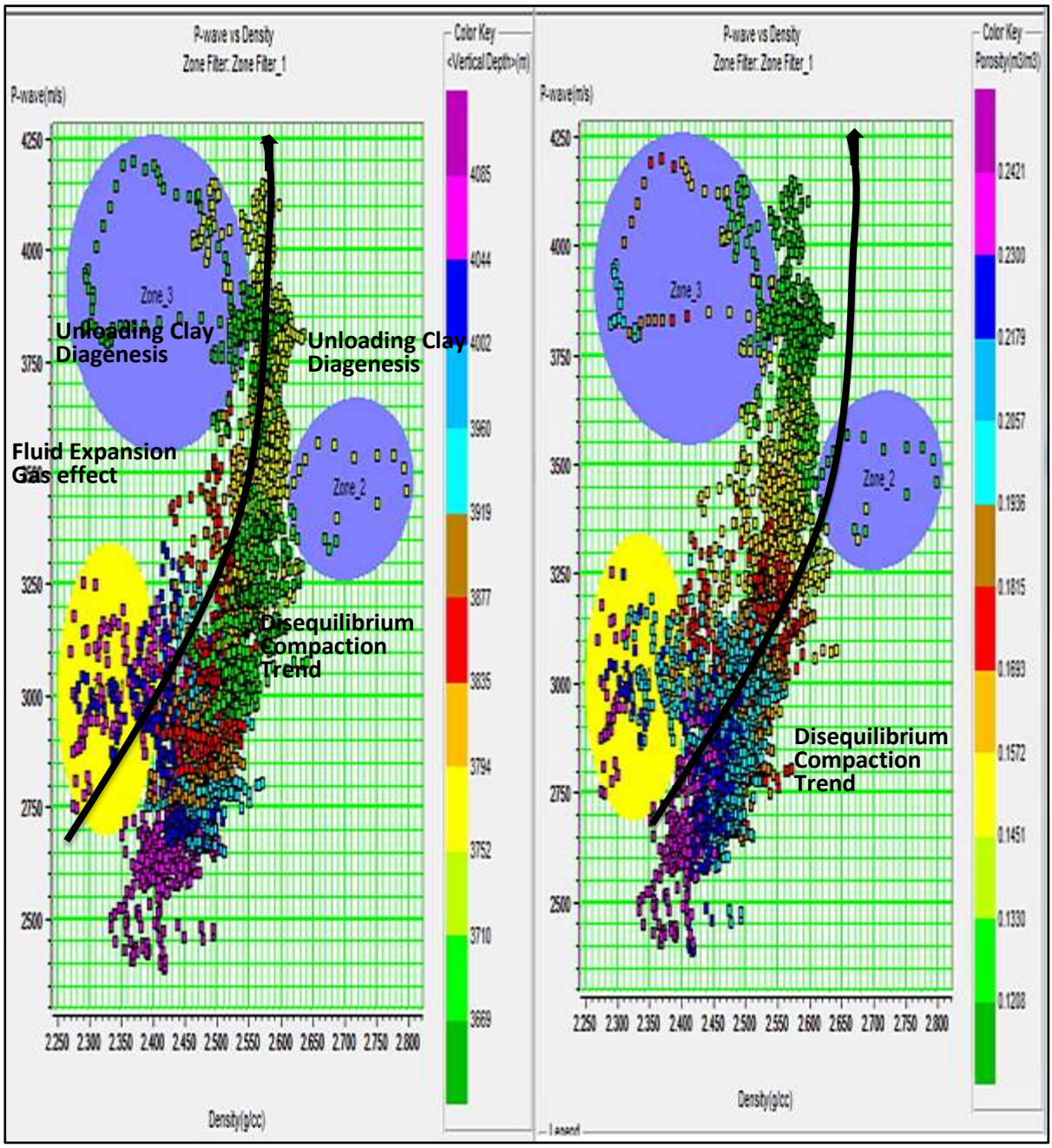

Figure 9- plot range of 3500 m to end of well of P-wave against density log.

The acoustic impedance in a normal depositional trend is expected to increase with depth, since it is the product of P-wave and density in a given layer. As sedimentation becomes denser (increase in density due to compaction) P wave increases, and the compact nature of the sediments brings about reduction in the pore space in the formation. Considering figure 10, the cross plot discloses an increase in the acoustic impedance and a reduction in porosity with respect to depth, up to depth of about 3700 m, as the arrow reveals the compaction trend pattern. Sediments at about 3700 and above (yellow circle) show a reduction in acoustic impedance and a significant increase in porosity against the clusters of sediments above them. The vertical depth is used as the color key.

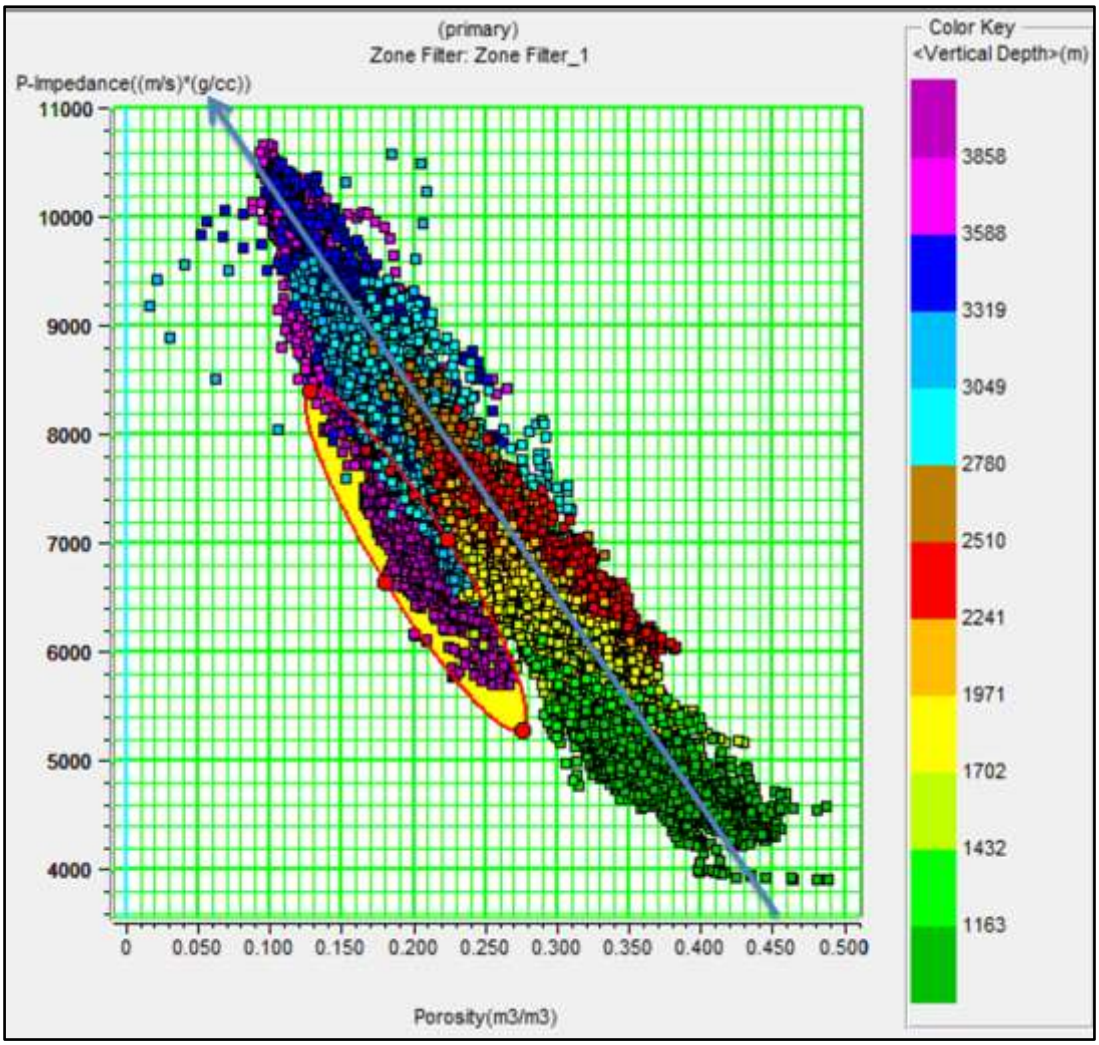

Figure 10-The cross plot of P-impedance versus porosity.

Conclusions

Disequilibrium compaction, also regarded as under-compaction, is identified as a major mechanism of abnormal pore pressure in this sedimentary formation, as experienced from the results analysis. Density and acoustic wave increase with increased depth of burial due to compaction of sediments. However, under-compaction plays a significant role from the point of reversal from the normal compaction trend line with the implication of reduction in density and acoustic wave with respect to burial depth. The analysis from the point of reversal discloses that the selected interval experience san abnormal pore pressure regime because of disequilibrium compaction, unloading, clay diagenesis and fluid expansion that have been identified as the major causes of abnormal pore pressure in the formation.

References

1. Swarbrick, R.E., Osborne, M.J. **1998.** Mechanisms that generate abnormal pressures: an overview, in Law, B.E., G.F. Ulmishek, and V.I. Slavin eds., Abnormal pressures in hydrocarbon environments: *AAPG Memoir*, **70**: 13–34.
2. Huffman, A. R. **2002.** The Future of Pressure Prediction Using Geophysical Methods, in Huffman A.R. and Bowers, G. L. editors, Pressure Regimes in Sedimentary Basins and Their Prediction, *AAPG Memoir*, **76**: 217-233.
3. Opara, A. I. **2010**. Origin and Generation Mechanisms of Geopressures in Shale Dominated Settings World-Wide: *A Review Global Journal of Pure and Applied Sciences Bachudo Science* Co. Ltd Printed in Nigeria. Issn 1118-0579, **16**(4): 429- 438.

4. Tuttle, M. L. W., Charpentier R. R. and Brownfield, M. E. **1999**. The Niger Delta Petroleum System: Niger Delta Province, Nigeria, Cameroun and Equatorial Guinea, Africa: *USGS Open-File Report* 99 - 50H.

5. Kulke, H. **1995**. Nigeria Regional Petroleum Geology of the World Part II (Eds. Kulke, H): Africa, America, Australlia and Antarctica: Berlin, *Gebruder Borntraeger*, **11**: 143-172.

6. Ekweozor, C. M. and Daukoru, E.M. **1994**. Petroleum Source Bed Evaluation of Tertiary Niger Delta--reply: *American Association of Petroleum Geologists Bulletin*, **68**: 390-394.

7. Lehnar, P. and De Ruiter, P.A.C. **1977**. Structural History of Atlantic Margin of Africa *AAPG Bulletin*, **16**: 961 – 981.

8. Evamy, B. D., Haremboure, J., kamerling, P., Knaap, W. A., Molloy, F. A., and Rowlaands, P. H. **1978**. Hydrocarbon Habit of Tertiary Niger Delta: *America Association of Petroleum Geologists Bulletin*, **62**: 277-298

9. Xiao, H. and Suppe, J. **1992**. Origin of Rollover, *AAPG Bulletin*, **76**: 509-529.

10. Short, K. C. and Stauble, A.J. **1965**. Outline of geology of Niger Delta: *American Association of Petroleum Geologists Bulletin*, **51**:761-779.

11. Weber, K. J. and Daukoru, E.M. **1975**. *Petroleum Geology of the Niger Delta*: Proceedings of the 9th World Petroleum Congress: Applied Science Publishers, Ltd, London, **2**: 210- 221.

12. Doust, H. and Omatsola, E. **1990**. Niger Delta. In: Divergent and Passive Margin Basins (Eds. Edwards. P. A. and Santogrossi, P.A.). *The American Association of Petroleum Geologist*, Tulsa, USA, **48**: 239-238.

13. D.O Ogagure **2008**. Localized Vp-Vs Relationship for the Niger Delta Sediments. *Pacific Journal of Science and Technology*. **9**(2): 558-561 (2008)

14. Coates, G.R and Dumanoir, J. L. **1973**. A new Approach to Improved Log Derived Permeability, Proceedings of the *SPWLA* 14th Annual Logging Symposium held in Lafayette May 6-9, 1 - 28

15. O'Conner, S., R. E. Swarbrick, and R. W. Lahann, **2011**. Geologically driven pore fluid pressure models and their implications for petroleum exploration. Introduction to thematic set: *Geofluids*, **11**: 343–348, doi:10.1111/j.1468-8123.2011.00354.x.